IEEE Photonics Journal
An IEEE Photonics Society Publication

Open Access

Minimizing the Number of Spans for Terrestrial Fiber-Optic Systems Using Quasi-Single-Mode Transmission

Volume 10, Number 1, February 2018

Jian Zhao
Inwoong Kim
Olga Vassilieva
Tadashi Ikeuchi
Wei Wang
He Wen
Guifang Li

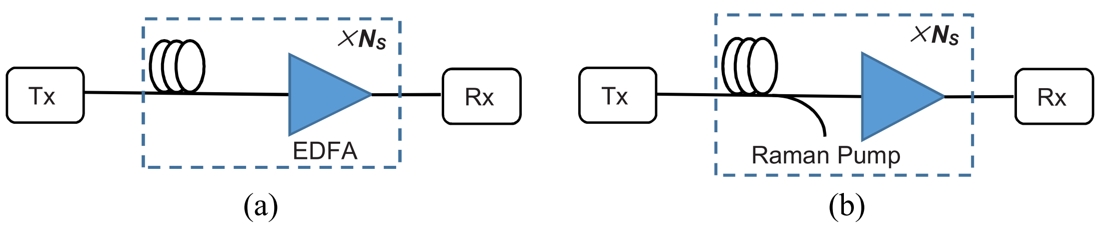

DOI: 10.1109/JPHOT.2017.2778218

Minimizing the Number of Spans for Terrestrial Fiber-Optic Systems Using Quasi-Single-Mode Transmission

Jian Zhao,[1] Inwoong Kim,[2] Olga Vassilieva,[2] Tadashi Ikeuchi,[2] Wei Wang,[1] He Wen,[3,1] and Guifang Li[3,1]

[1]Key Laboratory of Opto-Electronic Information Technical Science of Ministry of Education, School of Precision Instruments and Opto-Electronics Engineering, Tianjin University, Tianjin 300072, China
[2]Fujitsu Laboratories of America, Inc., Richardson, TX 75082 USA
[3]CREOL, The College of Optics and Photonics, University of Central Florida, Orlando, FL 32816 USA

DOI:10.1109/JPHOT.2017.2778218

Manuscript received October 18, 2017; revised November 17, 2017; accepted November 25, 2017. Date of publication December 6, 2017; date of current version December 27, 2017. This work was supported in part by the National Basic Research Program of China (973) through Project 2014CB340104, in part by the National Science Foundation China through Projects 61307085 and 61377076, in part by Open Fund of the Key Laboratory of Optical Information Science and Technology (Nankai University), in part by the China Scholarship Council through Project 201506255103, and in part by Tianjin Education Commission through Project 20110704. Corresponding authors: Jian Zhao and Guifang Li (e-mail: enzhaojian@tju.edu.cn; li@creol.ucf.edu).

Abstract: We show that quasi-single-mode transmission in few-mode fibers (FMFs) can reduce the number of spans for a fixed transmission distance and, consequently, the cost per bit for terrestrial transmission systems by minimizing both the Capex and Opex. The Gaussian-noise model is employed to estimate the nonlinear noise power spectral density both, which depends on the effective area of the FMF and span length, for Er-doped fiber amplifier (EDFA) and hybrid Raman/EDFA systems. Together with amplified spontaneous emission noise, an optical signal-to-noise ratio (OSNR) for a fixed transmission distance as a function of the effective area of the FMF and span length can be obtained. Given a target OSNR for a particular modulation format, we determine the maximum span length or the minimum number of spans as the effective area of the FMF varies both analytically and through numerical simulations. The effect of multipath interference in the FMF on the minimum number of span has also been investigated.

Index Terms: Quasi-single-mode (QSM), coherent optical communications, Gaussian-noise (GN) model, nonlinear interference, multipath interference (MPI).

1. Introduction

Data traffic has been grown exponentially in the past decades and this trend is expected to continue for the foreseeable future. According to the most recent data traffic forecast [1], global mobile data traffic is expected to increase sevenfold between 2016 and 2021. Mobile network connection speeds will increase threefold by 2021. The continued growth of data traffic has led to the development of high-speed optical communication systems with high spectral efficiency and overall capacity [2]–[4]. The most recent technology deployed commercially is digital coherent optical transmission [5]. The development of fast ADC and DAC together with digital signal processing (DSP) algorithms has

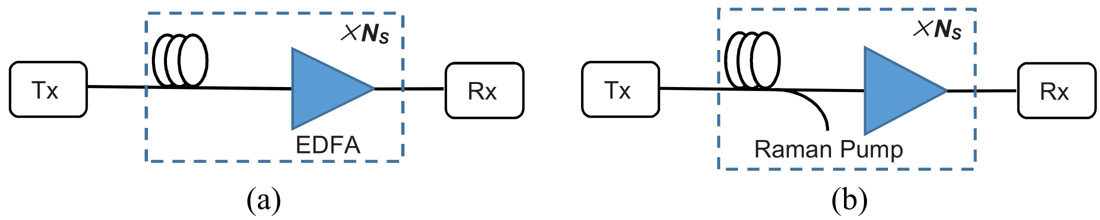

Fig. 1. (a) Lumped amplification (EDFA only) and (b) hybrid amplification optical fiber transmission system. N_s is the number of spans.

enabled coherent transmission to become the dominant technique. The increase in the capacity of digital coherent optical transmission is mainly due to two factors. First digital coherent optical transmission allows near-perfect compensation of linear impairments such as chromatic dispersion (CD) and polarization mode dispersion (PMD) [6]. Second, coherent transmission allows shot-noise limited detection and power-efficient coding, minimizing the launch power and, as a result, fiber nonlinear impairments. Fiber nonlinearity can also be compensated using digital backpropagation (DBP) or, alternatively, be reduced using quasi-single-mode (QSM) transmission in few-mode fibers (FMF) [7]. These advanced techniques have been almost extensively investigated for undersea systems.

With the high-rate of increase in internet bandwidth demand, the need for reducing the cost per bit for optical transport will become ever more imperative. Since the transmission distance for terrestrial systems is much shorter than undersea systems, it would be wise to investigate whether QSM in FMFs could be utilized to reduce the cost per bit for terrestrial optical transport. In this paper, we show that QSM transmission in FMFs can reduced the number of spans for a specific transmission distance and thus overall cost per bit. This is brought about by reducing the number of spans (or amplifier sites) for the specific transmission distance. Fewer amplifiers not only lead to the reduction of capital expenses (Capex) but also operational expenses (Opex).

This paper is organized as follows. In Section 2, we present the system model used in this work, which can be described by the GN model [8]–[10]. In Sections 3 and 4, we present the dependence of the minimum number of spans on the effective area of the fundamental mode of the FMF for systems with lumped amplification and hybrid amplification (HA), respectively. In Section 5, we evaluate the effect of multipath interference (MPI) [11], [12] on the minimum number of spans. Finally, in Section 6 we summarize the main conclusions of this paper.

2. System Model

We consider typical wavelength-division multiplexed (WDM) optical transmission systems shown in Fig. 1. The GN model is utilized to analyze the system performance. To do so, we assume that the transmitted signal is a comb of Nyquist WDM channels, with channel spacing approaching the symbol rate, whose power spectral density (PSD) is essentially flat. Such a spectrum can be realized using polarization-multiplexed M-ary quadrature-amplitude modulation (QAM) with spectral shaping. Let N_{ch} be the number of WDM carriers, R_s symbol rate, Δf the channel spacing, the total occupied bandwidth is $B = N_{ch}\Delta f$. In this study, we set the symbol rate at 32 Gbaud, channel spacing at 32 GHz. With a total of 125 channels in the C band on a 32 GHz grid, the total bandwidth of the WDM channels is B = 4 THz.

We consider QSM using FMFs as transmissions fibers, which are highly dispersive and uncompensated optically. Only the fundamental mode of the FMF is used for the optical transmission of the WDM signals. The effective area of the fundamental mode A_{eff} in this study ranges from 80 μm^2 corresponding to SSMF to 480 μm^2. This effective area (480 μm^2) for the fundamental mode of a FMF can be realized in a step-index design with core (cladding) index of 1.446 (1.444) and a core radius of 22.2 μm. The effective index difference between the fundamental mode and the first high-order mode is $>5\times10^{-4}$ to ensure low mode crosstalk. The required effective index difference of $>5\times10^{-4}$ for weak coupling between the fundamental mode and the LP_{11} mode is on the same order as that between the two polarizations of polarization-maintaining fibers [13]. The chromatic dispersion coefficient is assumed to be D = 20 ps/nm/km. For simplicity of the first study of this kind, we shall assume that the span length L_{span} is uniform and fiber loss is perfectly compensated by either Er-doped fiber amplifiers (EDFA) as shown in Fig. 1(a), or the combination of EDFAs and Raman amplifiers (RA) as shown in Fig. 1(b). These amplification schemes result in differences in the amplified spontaneous emission noise as well as the nonlinear interference (NLI) noise. The total transmission distance L_{total} is set at 3,000 km. The goal of this study is to determine the dependence of span length, and therefore, the number of spans or amplification sites, on the effective area of the FMF for these systems configurations. The results can serve as a guideline for the future development of cost-effective coherent terrestrial optical transport systems.

3. QSM Using Lumped EDFAs

In QSM using lumped EDFAs shown in Fig. 1(a), the linear noise comes from the amplified spontaneous emission (ASE) of EDFAs. The ASE power spectral density (PSD) for each amplifier in two polarizations is given by

$$N_{\text{ASE}} \approx 2n_{sp}\cdot h\nu_0\cdot G = NF\cdot h\nu_0\cdot G \tag{1}$$

where NF is the noise figure of the EDFA, $h\nu_0$ is the photon energy at the operating frequency ν_0 and h is Planck's constant, $G\gg 1$ is the gain of the EDFA which is assumed to be equal to the total loss of a span $G_{dB}=\alpha_{dB}L_{\text{span}}$, α_{dB} is the fiber loss coefficient in units of decibels per unit distance.

According to the GN model, the nonlinear noise originating from nonlinear interference (NLI) can be well approximated as additive white Gaussian noise (AWGN). For a large number of WDM channels, the NLI scales linearly with the number of spans and the cube of the signal power per channel P_{ch}. The NLI PSD introduced in each fiber span can be expressed as [9]:

$$N_{\text{NLI}} \cong \Gamma_{NLI}\cdot\frac{S_{ch}^3}{E_{ph}^2} \tag{2}$$

where $E_{ph}=h\nu_0$ is the photon energy, $S_{ch}=P_{ch}/R_s$ is the PSD of transmitted channels which is flat in accordance to Nyquist shaping and Γ_{NLI} is the normalized NLI efficiency which depends on the parameters of the link and signal, and independent of the modulation format, according to [8]:

$$\Gamma_{NLI} \cong E_{ph}^2\frac{8}{27}\frac{\gamma^2 {L_{eff}}^2}{\pi\beta_2 L_{eff,a}}a\sinh\left(\frac{\pi^2}{2}\beta_2 L_{eff,a}B_{ch}^2 N_{ch}^{2\frac{B_{ch}}{\Delta f}}\right) \tag{3}$$

where $\gamma=\frac{2\pi}{\lambda}\frac{n_2}{A_{eff}}$ is the fiber nonlinear coefficient and is set as 1.3/W/km at 1550 nm for SMF, n_2 is the nonlinear index of refraction, $\beta_2=-\frac{c}{2\pi\nu_0^2}D$, $L_{eff,a}=1/\alpha$ is the asymptotic effective length, Δf is channel spacing, N_{ch} is the number of channels, B_{ch} is the channel bandwidth. Given the long span length considered in this paper, we can set $L_{eff}\approx L_{eff,a}$

The PSD of total noise at the receiver is

$$N_{\text{Rx}} = N_s(N_{ASE}+N_{NLI})+N_{\text{Booster}} \tag{4}$$

where N_s is the number of spans. For simplicity, the ASE noise of the booster EDFA in the transmitter is assumed to be the same as the in-line amplifier, so

$$N_{\text{Rx}} = (N_s+1)\cdot N_{ASE}+N_s\cdot N_{NLI} \tag{5}$$

The optical signal-to-noise ratio (OSNR), taking into account both ASE noise and NLI, can be expressed as:

$$\text{OSNR} = \frac{P_{ch}}{2P_{ASE}+P_{NLI}} = \frac{S\cdot R_s}{\left[(N_s+1)NF\cdot\exp\left(\frac{\alpha L_{\text{total}}}{N_s}\right)+N_s\Gamma_{NLI}\cdot S^3\right]\cdot B_{ref}} \tag{6}$$

where P_{ASE} is the ASE noise power of per polarization, $S = S_{ch}/E_{ph}$ is the normalized PSD per channel expressed as average number of photons per symbol, $B_{ref} = 0.1$ nm is the reference bandwidth for OSNR. Since both the linear noise and the signal power per span increases exponentially with span length, a target OSNR, OSNR_T corresponding to a specific BER threshold can only be achieved if the span length (number of spans) does not exceed a certain length (fall below a minimum value $N_{s,\min}$).

To obtain the minimum number of spans $N_{s,\min}$, (6) can be solved numerically. Fortunately, a closed form analytical solution can also be found. Equation (6) can be arranged as a polynomial equation in S with the parameters of the transmission link and the target OSNR, OSNR_T as parameters as follows:

$$S^3 + pS + q = 0 \tag{7}$$

with

$$p = -\frac{1}{(\mathrm{OSNR}_T \cdot B_{ref}/R_s) \cdot N_s \cdot \Gamma_{NLI}},\ q = \frac{(N_s+1)NF}{N_s \Gamma_{NLI}} \exp\left(\frac{\alpha L_{\text{total}}}{N_s}\right).$$

From a physical point of view, there should be only one value of S that would result in the minimum number of spans, $N_{s,\min}$. That is, (7) should admit only one real root, which requires that the discriminant of (7)

$$\Delta = (q/2)^2 + (p/3)^3 = \frac{(N_s+1)^2 NF^2}{4{N_s}^2 \Gamma_{NLI}^2} \exp\left(\frac{2\alpha L_{\text{total}}}{N_s}\right) - \frac{1}{27(\mathrm{OSNR}_T \cdot B_{ref}/R_s)^3 N_s^3 \Gamma_{NLI}^3} \tag{8}$$

be positive. At the critical condition, $N_s = N_{s,\min}$ and the discriminant vanishes:

$$N_{s,\min}(N_{s,\min}+1)^2 \exp\left(\frac{2\alpha L_{\text{total}}}{N_{s,\min}}\right) - \frac{4}{27NF^2(\mathrm{OSNR}_T \cdot B_{ref}/R_s)^3 \Gamma_{NLI}} = 0 \tag{9}$$

In the following, we will present the minimum number of spans for a fixed total transmission distance L_{total} of 3000 km as a function of the effective area A_{eff}, which plays an important role in NLI, with fiber loss as a parameter. The noise figure NF of EDFAs is set at 5 dB. In this work, we focus on the PM-QPSK modulation format and set BER = 3.8e-3, the 7% hard-decision (HD) advanced FEC threshold. For PM-QPSK modulation format, the SER can be estimated by:

$$SER = erfc\left(\sqrt{\frac{E_s}{4N_0}}\right) = erfc\left(\sqrt{\mathrm{OSNR}\frac{B_{ref}}{2R_s}}\right) \tag{10}$$

With gray coding, $BER = SER/\log_2 M$ and is related to the OSNR by:

$$\mathrm{OSNR} = \frac{2R_s}{B_{ref}}[erfc^{-1}(2BER)]^2 \tag{11}$$

Fig. 2(a) shows the minimum number of spans versus the effective area of the fiber with fiber loss coefficients of 0.20 dB/km, 0.18 dB/km and 0.16 dB/km, respectively. The attenuation of FMFs is similar to that of SMFs at the 1550 nm. The loss of a FMF demonstrated in [7] was 0.16 dB/km. In Fig. 2(a), the numerical results for $\lfloor N_{s,\min} \rfloor$, shown as scatter plots, were obtained from (6) and the analytical results for $\lfloor N_{s,\min} \rfloor$, shown in solid lines, were calculated from (9). The results of numerical calculation and analytical solution agree with each other very well. Even though $N_{s,\min}$ can only take on integer values $\lfloor N_{s,\min} \rfloor$, the optimum launch power per channel, P_{ch}, does change continuously as the effective area of the fiber increases, as shown in Fig. 2(b). As can be seen in Fig. 2(a), the minimum number of spans decreases as A_{eff} increases, making a strong case for QSM transmission. Starting from the small A_{eff} of SSMF, the $N_{s,\min}$ reduces quickly with increasing A_{eff}. The minimum number of spans decrease from 24 to 18 with A_{eff} increasing from 80 μm^2 to 480 μm^2 for a fiber loss of 0.20 dB/km. The corresponding span lengths increase from 125 km to 167 km. As expected, the minimum number of spans also decrease with the loss coefficient. For example, the minimum numbers of spans are 15 and 13 at $A_{eff} = 480\,\mu$m^2 for a loss coefficient of

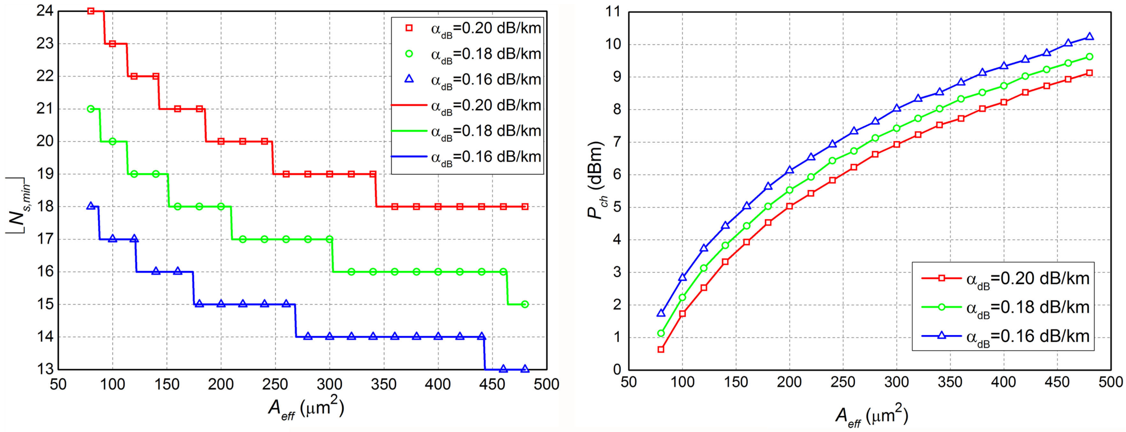

Fig. 2. Numerical calculation (scatter plot) and analytical solution (solid line) of (a) the minimum number of spans and (b) the optimum power corresponding to (a) versus A_{eff} from 80 to 480 μm^2 with different fiber loss coefficients for lumped amplification.

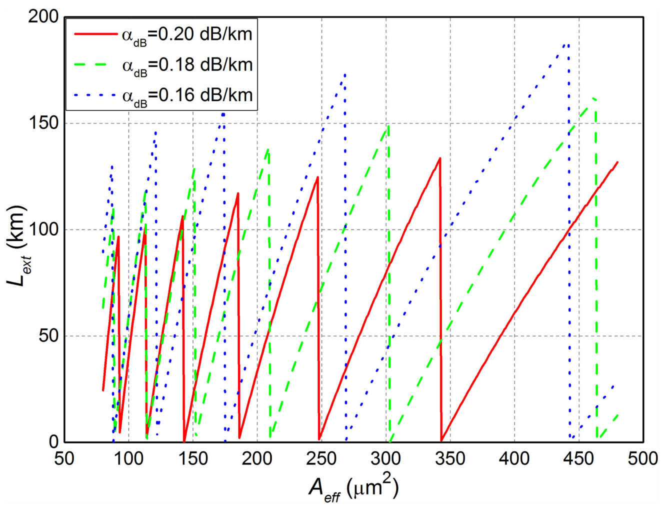

Fig. 3. L_{ext} of a 3000-km lumped amplification system versus A_{eff} from 80 to 480 μm^2 using the minimum number of spans given in Fig. 2(a) and optimized input power given in Fig. 2(b).

0.18 dB/km and 0.16 dB/km, respectively. The minimum number of spans of 13 for a loss coefficient to 0.16 dB/km corresponds to a span length of 230 km using EDFA only. This demonstrates the benefit of utilizing QSM to enable long span length in EDFA-only systems.

As shown in Fig. 2(a), $\lfloor N_{s,\min} \rfloor$ varies in a staircase fashion as A_{eff} increases. In each flat region, the system OSNR margin does increase as a result of large effective areas. This OSNR margin can be used to extend the total transmission distance L_{total} over 3000 km. From (6), L_{total} extension due to the increased OSNR margin can be calculated as:

$$L_{ext} = \frac{\lfloor N_{s,\min} \rfloor}{\alpha} \ln\left(\frac{S}{(\lfloor N_{s,\min} \rfloor + 1)(\text{OSNR}_T \cdot B_{ref}/R_s) NF} - \frac{\lfloor N_{s,\min} \rfloor \Gamma_{NLI} S^3}{(\lfloor N_{s,\min} \rfloor + 1)^2 NF} \right) - L_{\text{total}} \tag{12}$$

We compute the L_{ext} as a function of the effective area of the fiber, as shown in Fig. 3, using the minimum number of spans given in Fig. 2(a) and optimum power given in Fig. 2(b). For a fiber with a loss of 0.16 dB/km, the system margin is almost 190 km if the effective area of the fiber is increased to $A_{eff} = 440\ \mu\mathrm{m}^2$ yielding a total distance of 3190 km with only 13 spans.

4. QSM Using Hybrid Amplification

Hybrid amplification as shown in Fig. 1(b) is expected to further increase (reduce) the span length (the number of spans). Hybrid amplification reduces the linear noise due to Raman amplification and nonlinear noise by reducing the path-averaged power. In what follows we evaluate both the linear and nonlinear noise for HA.

With backward-pumped Raman amplification, pump depletion is negligible and, as a result, small-signal gain can be used regardless of the launch power in each span. Specifically, the small-signal Raman gain profile $G_{RA}(z)$ is given by [14]:

$$G_{RA}(z) = \exp\left\{\int_0^z C_R P_{\mathrm{pump}} \exp[-\alpha_p(L_{\mathrm{span}} - \xi)]d\xi\right\} \tag{13}$$

where $C_R = g_R/A_{eff}$ with $g_R = 0.33 \times 10^{-13}$ m/W over the C band, α_p is the fiber attenuation coefficient at the pump wavelength which is 0.1 dB/km higher than at the signal wavelength. The on-off Raman gain is $G_{RA,\mathrm{on-off}} = G_{RA}(z = L_{\mathrm{span}})$. Taking the noise characteristics of the EDFA and Raman amplifier together, the equivalent noise figure of the hybrid amplifier is given by

$$NF_{HA,eq} = NF_{RA,eq} + \frac{NF_{EDFA} - 1}{G_{RA,\mathrm{on-off}}} \tag{14}$$

where $NF_{RA,eq}$ is the equivalent noise figure of the Raman amplifier [15].

The normalized NLI efficiency $\Gamma_{NLI,HA}$, in general, depends on the Raman gain profile. Under the undepleted-pump assumption, the NLI efficiency is also independent of the input power, and is given by

$$\Gamma_{NLI,HA}(L_{\mathrm{span}}) = \frac{256}{27}\gamma^2 E_{ph}^2 \int_0^{\frac{B_{opt}}{2}} \nu R(\nu) \log\left(\frac{B_{opt}}{2\nu}\right) d\nu \tag{15}$$

where $R(\nu)$ is the generalized four-wave mixing efficiency [15], which depends on the loss and Raman gain profile $G_{RA}(z)$ according to:

$$R(\nu, L_{\mathrm{span}}) = \left|\int_0^{L_{\mathrm{span}}} 10^{-\frac{\alpha_{dB}}{10}z} G_{RA}(z)\, e^{j4\pi^2\beta_2\nu^2 z} dz\right|^2 \tag{16}$$

and β_2 is the fiber dispersion coefficient and ν is among the transmission band.

In this paper, we assume that the Raman gain accounts for 55% of the span loss in dB [16]. Fig. 4 plots the NLI efficiency as a function of span length. It is observed that the normalized NLI efficiency is almost flat for span lengths over 100 km. Specifically, $\Gamma_{NLI,HA}$ varies by 0.11 dB for span lengths ranging from 100 to 300 km. Since the span length in our study falls within this range, we assume that the normalized NLI efficiency in HA system is a constant from now on.

The OSNR of the hybrid amplification system is given by:

$$\mathrm{OSNR} = \frac{S \cdot R_s}{\left[(N_s + 1)NF_{HA,eq}(N_s) \cdot \exp\left(\frac{\alpha L_{\mathrm{total}}}{N_s}\right) + N_s \Gamma_{NLI,HA} \cdot S^3\right] \cdot B_{ref}} \tag{17}$$

from which the minimum number of spans can be calculated using the same procedure as in Section 3. The NF of HA system is a function of span length and does not a constant any more. Fig. 5 plots the minimum number of spans as a function of A_{eff} for hybrid amplification. The minimum span decreases with the increase of A_{eff}. It is observed that the minimum number of spans for hybrid amplification systems is significantly decreased in comparison with lumped-amplification systems. For example, $\lfloor N_{s,\min} \rfloor$ is decreased from 18 to 14 at $A_{eff} = 480\ \mu\mathrm{m}^2$ and 0.20 dB/km loss. The minimum number of spans is only 11 at $A_{eff} = 480\ \mu\mathrm{m}^2$ and 0.16 dB/km loss. The L_{ext} of a 3000 km hybrid amplification system is shown in Fig. 6. For instance, for a FMF with a loss of

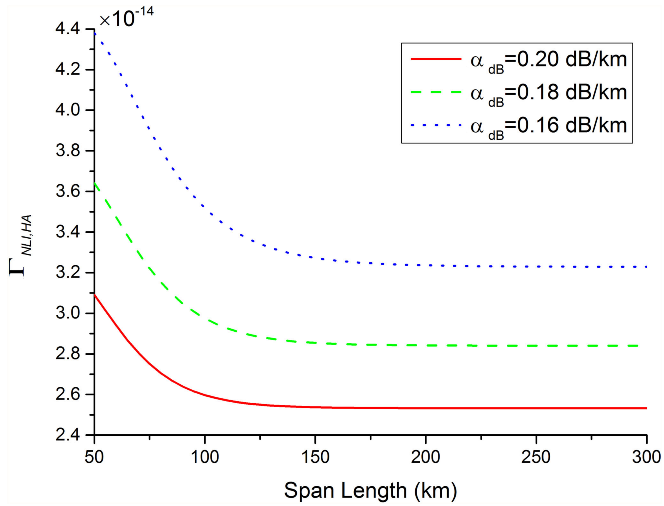

Fig. 4. Normalized NLI efficiency versus span length up to 300 km for hybrid amplification systems.

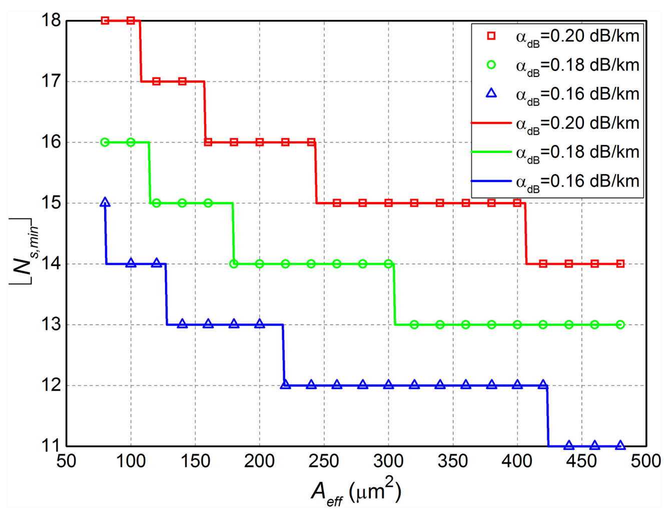

Fig. 5. Numerical calculation (scatter plot) and analytical solution (solid line) of the minimum number of spans versus A_{eff} from 80 to 480 μm^2 with different fiber loss coefficients for the hybrid amplification system.

0.16 dB/km, the total system length L_{total} can be increased by almost 220 km for an effective area of little larger than 400 μm^2, yielding an distance of 3220 km with only 11 spans.

5. The Effect of MPI

Multipath interference (MPI) is a potential impairment in QSM systems. In the weakly coupled regime, the effect of MPI arising from high-order modes can be neglected [17]. The mode crosstalk due to splicing is not considered in our model [18]. The MPI defined as the ratio of the total power of crosstalk to the average signal power accumulated within a single span can be written as [11]:

$$MPI = \frac{\Delta\alpha \cdot L - 1 + e^{-\Delta\alpha \cdot L}}{\Delta\alpha^2}\kappa^2 \tag{18}$$

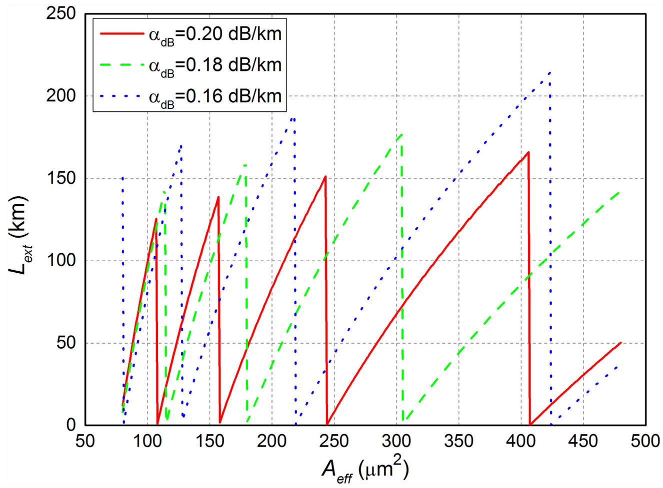

Fig. 6. L_{ext} of a 3000-km hybrid amplification system versus A_{eff} from 80 to 480 μm^2 using the minimum number of spans given in Fig. 5.

where $\Delta\alpha = \alpha_{11} - \alpha_{01}$ is the differential mode attenuation (DMA) between the attenuation coefficients α_{01} and α_{11} of the two lowest-order modes of the FMF [19], κ is the average power-coupling coefficient which describes the coupling strength between these two modes. We assume here that MPI due to other higher-order modes are negligible. In the following analysis, the DMA is set at 0.1 dB/km, and κ is set to 1e^{-3}/km. MPI is a linear impairment, and in theory, can be completely compensated. Indeed, complete MPI compensation has indeed been demonstrated in practice using equalization filters with sufficient tap lengths [7]. Of course, a longer tap length translates to a larger gate count and higher power consumption for the DSP chip. It is therefore valuable evaluate the effect of incomplete MPI compensation on the minimum number of spans. Including MPI, [12], the OSNR can be expressed as:

$$\mathrm{OSNR} = \frac{S \cdot R_s}{\left[(N_s + 1) \cdot NF_{HA,eq}(N_s) \cdot \exp\left(\frac{\alpha L_{\text{total}}}{N_s}\right) + N_s \cdot MPI(N_s) \cdot S + N_s \Gamma_{NLI,HA} S^3\right] \cdot B_{ref}} \tag{19}$$

An analytical solution for the minimum number of spans $N_{s,\min}$, to reach a target OSNR$_T$, include the effect of MPI, is still possible. Similar to (9), the polynomial equation for the per-channel S can be expressed as following:

$$S^3 + \frac{N_s \cdot (\mathrm{OSNR}_T \cdot B_{ref}/R_s) \cdot MPI(N_s) - 1}{N_s \cdot (\mathrm{OSNR}_T \cdot B_{ref}/R_s) \cdot \Gamma_{NLI,HA}} S + \frac{(N_s + 1) NF_{HA,eq}(N_s)}{N_s \Gamma_{NLI,HA}} \cdot \exp\left(\frac{\alpha L_{\text{total}}}{N_s}\right) = 0 \tag{20}$$

where

$$p = \frac{N_s \cdot (\mathrm{OSNR}_T \cdot B_{ref}/R_s) \cdot MPI(N_s) - 1}{N_s \cdot (\mathrm{OSNR}_T \cdot B_{ref}/R_s) \cdot \Gamma_{NLI,HA}}, \; q = \frac{(N_s + 1) NF_{HA,eq}(N_s)}{N_s \Gamma_{NLI,HA}} \cdot \exp\left(\frac{\alpha L_{\text{total}}}{N_s}\right).$$

At the critical condition, $N_s = N_{s,\min}$ and the discriminant of (20) vanishes

$$\begin{aligned}\Delta = \left(\frac{q}{2}\right)^2 + \left(\frac{p}{3}\right)^3 = \frac{(N_{s,\min} + 1)^2 NF_{HA,eq}{}^2(N_{s,\min})}{4N_{s,\min}{}^2 \Gamma_{NLI,HA}{}^2} \exp\left(\frac{2\alpha L_{\text{total}}}{N_{s,\min}}\right) + \frac{MPI^3(N_{s,\min})}{27\Gamma_{NLI,HA}{}^3} \\ - \frac{MPI^2(N_{s,\min})}{9N_{s,\min} \cdot (\mathrm{OSNR}_T \cdot B_{ref}/R_s) \cdot \Gamma_{NLI,HA}{}^3} + \frac{MPI(N_{s,\min})}{9N_{s,\min}{}^2 \cdot (\mathrm{OSNR}_T \cdot B_{ref}/R_s)^2 \cdot \Gamma_{NLI,HA}{}^3} \\ - \frac{1}{27N_{s,\min}{}^3 \cdot (\mathrm{OSNR}_T \cdot B_{ref}/R_s)^3 \cdot \Gamma_{NLI,HA}{}^3} = 0\end{aligned} \tag{21}$$

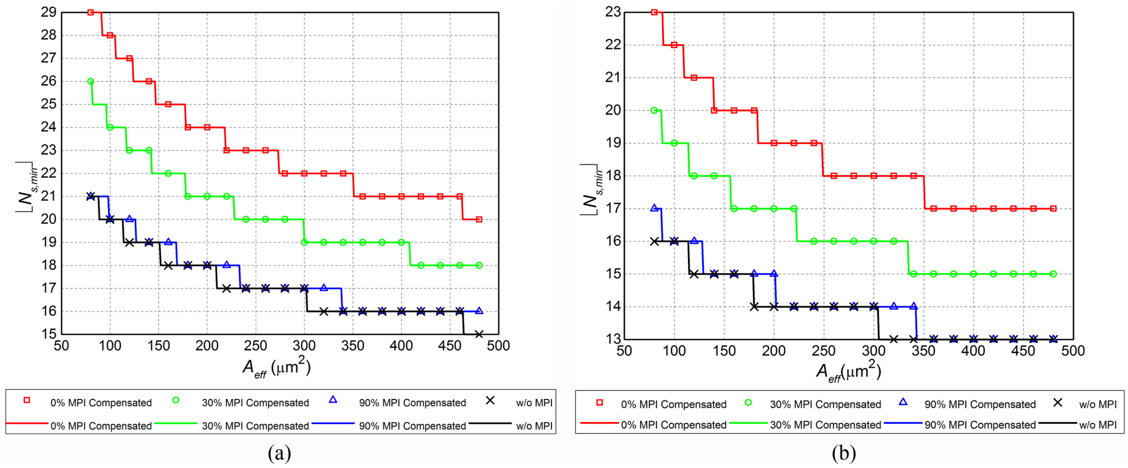

Fig. 7. Simulation (scatter plots) and analytical (solid line) results for (a) EDFA lumped and (b) EDFA/RA Hybrid amplification systems with different MPI compensation levels.

The minimum number of spans as a function of the effective area including the effect of MPI for lumped and hybrid amplification are shown in Fig. 7(a) and (b), respectively, with different levels of MPI compensation for the case of $\alpha_{01} = 0.18$ dB/km. As can be seen, if not compensated, MPI causes the minimum number of spans to increase from 15 (13) to 20(17), for lumped and hybrid amplification respectively, at an effective area of $A_{eff} = 480\,\mu\text{m}^2$. Fortunately, if 90% of the MPI noise was compensated, the minimum number of spans does not increase for many A_{eff} values within the range under consideration.

6. Conclusion

We investigated minimizing the number of spans using quasi single-mode transmission in few-mode fibers to reduce Capex and Opex for optical transmission. An analytical solutions for the minimum number of spans as a function of system parameters was derived. The analytical solutions matched quite well with numerical simulations. Both lumped amplification and hybrid amplification are considered, including the effect of MPI. Our results indicated that, for a 3000 km 32 GBaud PM-QPSK coherent WDM transmission system, the minimum number of spans can be decreased from 24 (18) to 18 (14) when the effective area of the fiber increased from 80 μm^2 to 480 μm^2 at a loss of 0.20 dB/km using lumped (hybrid) amplification. MPI can have a strong influence on the minimum number of spans. Fortunately, if 90% of the MPI noise is compensated, the minimum number of span would not be affected by MPI. We expected that the results presented here will help drive down the Capex and Opex of optical transmission systems. Terrestrial systems typically have inhomogeneous span lengths. The method presented in this paper can be applied to such systems on a case by case basis.

References

[1] Cisco Visual Networking Index: Global Mobile Data Traffic Forecast Update, 2016–2021 White Paper, 2017. [Online]. Available: http://www.cisco.com/c/en/us/solutions/collateral/service-provider/visual-networking-index-vni/mobile-white-paper-c11-520862.html

[2] D. J. Richardson, "Filling the light pipe," *Science*, vol. 330, no. 6002, pp. 327–328, 2010.

[3] B. J. Puttnam *et al.*, "2.15 Pb/s transmission using a 22 core homogeneous single-mode multi-core fiber and wideband optical comb," in *Proc. Eur. Conf. Opt. Commun.*, 2015, Paper PDP.3.1.

[4] D. Soma *et al.*, "2.05 Peta-bit/s super-Nyquist-WDM SDM transmission using 9.8-km 6-mode 19-core fiber in full C band," in *Proc. Eur. Conf. Opt. Commun.*, 2015, Paper PDP3.2.

[5] G. Li *et al.*, "Space-division multiplexing: The next frontier in optical communication," *Adv. Opt. Photon.*, vol. 6, no. 4, pp. 413–487, 2014.

[6] G. Li, "Recent advances in coherent optical communication," *Adv. Opt. Photon.*, vol. 1, no. 2, pp. 279–307, 2009.

[7] Q. Sui *et al.*, "Long-haul quasi-single-mode transmissions using few-mode fiber in presence of multi-path interference," *Opt. Exp.*, vol. 23, no. 3, pp. 3156–3169, 2015.

[8] P. Poggiolini, "The GN model of non-linear propagation in uncompensated coherent optical systems," *J. Lightw. Technol.*, vol. 30, no. 24, pp. 3857–3879, Dec. 2012.

[9] V. Curri *et al.*, "Design strategies and merit of system parameters for uniform uncompensated links supporting Nyquist-WDM transmission," *J. Lightw. Technol.*, vol. 33, no. 18, pp. 3921–3932, Sep. 2015.

[10] P. Poggiolini, G. Bosco, A. Carena, V. Curri, Y. Jiang, and F. Forghieri, "The GN-model of fiber non-linear propagation and its applications," *J. Lightw. Technol.*, vol. 32, no. 4, pp. 694–721, Feb. 2014.

[11] J. D. Downie *et al.*, "Quasi-single-mode fiber transmission for optical communications," *IEEE J. Sel. Topics Quantum Electron.*, vol. 23, no. 3, May/Jun. 2017, Art. no. 4400312.

[12] M. Mlejnek, I. Roudas, J. Downie, N. Kaliteevskiy, and K. Koreshkov, "Coupled-mode theory of multipath interference in quasi-single mode fibers," *IEEE Photon. J.*, vol. 7, no. 1, Feb. 2015, Art. no. 7100116.

[13] C. Emslie, "Polarization maintaining fibers," in *Specialty Optical Fibers Handbook*, A. Méndez and T. F. Morse, Eds. Orlando, FL, USA: Academic, 2007, pp. 243–277.

[14] V. Curri, A. Carena, P. Poggiolini, G. Bosco, and F. Forghieri, "Extension and validation of the GN model for non-linear interference to uncompensated links using Raman amplification," *Opt. Exp.*, vol. 21, no. 3, pp. 3308–3317, 2013.

[15] V. Curri, "System advantages of Raman amplifiers," in *Proc. Nat. Fiber Opt. Eng. Conf.*, Denver, CO, USA, 2000, pp. 35–46.

[16] V. Curri and A. Carena, "Merit of Raman pumping in uniform and uncompensated links supporting NYWDM transmission," *J. Lightw. Technol.*, vol. 34, no. 2, pp. 554–565, Jan. 2016.

[17] N. Bai and G. Li, "Equalizer tap length requirement for mode group delay-compensated fiber link with weakly random mode coupling," *Opt. Exp.*, vol. 22, no. 4, pp. 4247–4255, 2014.

[18] Y. Jung *et al.*, "Adiabatically tapered splice for selective excitation of the fundamental mode in a multimode fiber," *Opt. Lett.*, vol. 34, no. 15, pp. 2369–2371, 2009.

[19] K. Ho and J. Kahn, "Mode-dependent loss and gain: statistics and effect on mode-division multiplexing," *Opt. Exp.*, vol. 19, no. 17, pp. 16612–16635, 2011.